RESEARCH PAPER

PCCP
www.rsc.org/pccp

Comparison of mesoscopic phospholipid–water models†

Marieke Kranenburg, Jean-Pierre Nicolas and Berend Smit*

Department of Chemical Engineering, University of Amsterdam, Nieuwe Achtergracht 166, 1018 WV Amsterdam, The Netherlands. E-mail: b.smit@science.uva.nl

Received 29th April 2004, Accepted 3rd June 2004
First published as an Advance Article on the web 23rd June 2004

In this study we show how a coarse-grained model of a phospholipid can be developed and we study the parameter sets applied to the formation of a coarse-grained dimyristoyl phosphatidyl choline (DMPC) bilayer. We create a model comprising a head group of three hydrophilic beads, to which two hydrophobic tails are connected. From results obtained with molecular dynamics simulations on a single lipid in water, a bond-bending potential between three subsequent beads was added. Using a bead volume of 90 Å^3, we reproduce the experimental values of the area per lipid and the hydrophobic thickness. There is no linear relation between the repulsion parameter a_{ij} and the level of coarse graining. The key factor in the formation of a lipid bilayer is the difference between the water–water and the water–hydrophobic tail repulsion parameters.

1. Introduction

In recent years many experimental techniques, such as X-ray crystallography, electron microscopy, infra-red and Raman spectroscopy, have been developed to characterize the structure of a membrane. Despite these developments, the precise functioning of membranes is still not well understood.[1] Therefore, a better characterization of the (phase) behavior of lipid membranes and the interaction between lipids and proteins is needed. This insight can be gained by performing computer simulations on detailed atomistic models based on realistic microscopic interactions.

The most used method to simulate biological systems, like lipid membranes, at an atomistic scale, is molecular dynamics (MD). In this method all interactions between the individual atoms are taken into account. However, these atomistic simulations cost a large amount of CPU time and thus these MD simulations are restricted to a small length or time scale. Recently the progresses in computational techniques and the increased power of computers have allowed us to reach time scales of 100 ns,[2,3] but there are still various phenomena, like for example phase transitions, that occur at longer time and length scales. These time and length scales are still not reachable by all-atom simulations and therefore other methods have been developed.

Although an all-atom model is seen as a realistic description of a biological membrane, one can always argue that even in such a model some details of the (quantum) chemical nature of the experimental system have been omitted. Similarly, one can assume that some of the atomic details can be ignored, while preserving the essential aspects of the molecular structure. In such a mesoscopic approach, clusters of atoms are, for example, replaced by spheres, which are connected by harmonic springs. The main advantage of mesoscopic simulations lies in the fact that the CPU time required for a simulation is lowered with 4 to 5 orders of magnitude. Therefore, many researchers have been interested in the question of how to coarse grain a phospholipid.[4–10]

A commonly used model is a coarse-grained MD simulation, where the interactions between the particles are defined by a Lennard-Jones type of potential.[4,7,9–11] However, if we consider particles that represent groups of atoms the centre of mass of these particles can overlap and therefore the Lennard-Jones interactions are often replaced with a soft repulsive force. These soft repulsive forces are often used in Dissipative Particle Dynamics (DPD) simulations. An important issue in these type of mesoscopic models is the relation with the underlying experimental system.

If we compare the different repulsion parameters that are used in the literature,[5,12–18] we see large differences and in most cases the intramolecular interactions are simple springs between DPD particles. In this work we study which factors are important in a mesoscopic model to reproduce the correct chain-length dependence of the area per lipid of a phospholipid bilayer. We showed in an earlier study[19,20] that a model, consisting of one hydrophilic head group particle and a single tail of hydrophobic beads, does not reproduce the correct phase behavior of a double tail lipid bilayer. In this work we show one can systematically derive a mesoscopic model of a phospholipid bilayer and investigate the various influences of the level of coarse graining, *i.e.* how many atoms are represented by a single DPD bead, and the choice of repulsion parameters. We compare two models that differ in the number of water molecules representing a single DPD particle and, additionally, we apply different sets of parameters. We develop our model by using all-atom MD simulations on a single lipid in water to obtain the missing intramolecular parameters of our mesoscopic model.

In this study we will focus on the formation of a bilayer of dimyristoyl phosphatidyl choline (DMPC) in the fluid or L_α phase and we will compare some structural properties of these bilayers with experiments and with MD simulations. In section 2 we describe the details of both the DPD and the MD simulations. In section 3.1 we discuss various models and parameter sets used by other groups applying DPD on amphiphilic systems and we present our models. In section 4 we show the density profiles computed with DPD simulations and we compare these with the profiles obtained with MD simulations and with experimental values.

2. Computational details

2.1. Molecular dynamics

Molecular dynamics (MD) simulations on an all-atom model of lipids and water were carried out to develop and test our

† Electronic supplementary information (ESI) available: Colour versions of Figs. 7 and 9. See http://www.rsc.org/suppdata/cp/b4/b406433j/

DOI: 10.1039/b406433j

mesoscopic model. For the development we used a single lipid in water and for the test a full bilayer. These MD simulations were carried out using the DLPOLY package.[21] An all-atom model was employed to describe the interactions between atoms using the potential energy parameter set PARAM27 from the CHARMM package.[22] The TIP3P water model[23] was used in all simulations. Bonds involving hydrogen were held fixed with the SHAKE algorithm.[24] Electrostatic interactions were computed using the Smooth Particle Mesh Ewald method.[25] Our simulations were performed in the *NVT* ensemble,[26] *i.e.* with constant number of particles (N), volume (V), and temperature (T). The equations of motions were solved using the Verlet Leapfrog integration algorithm[27] and simulations were run with periodic boundary conditions in all directions. All the simulations were performed using a cutoff radius of 12 Å for the van der Waals terms.

To simulate a single lipid in water, a lipid was equilibrated in vacuum. After this short equilibration, we added water to the system and let the system equilibrate, using the *NPT* ensemble. After this equilibration, we collected 20 independent starting configurations. For each configuration we performed *NVT* simulations at 300 K for 1 ns, with time step $\Delta t = 0.002$ ps, to obtain good statistics.

To simulate a lipid bilayer, we performed the following procedure. Initially, a single lipid molecule stretched along its longer axis was pre-equilibrated in vacuum. We built a complete membrane by placing the lipids on a 6×6 grid with hydrophilic head groups forming the outer side of the membrane and the aliphatic chains the inner side. The size of the grid is set such to get an area per lipid equal to the experimental value of 63 Å^2. The second layer of the membrane has been built by mirroring twice the initial lipid layer with respect to both the mid plane of the membrane and a perpendicular plane to conserve the chirality of the molecule. The dry membrane was equilibrated during a few hundred time steps. Subsequently, the box was filled by adding water molecules. The resulting simulation box of dimension $47.6 \times 47.6 \times L_z$, with $L_z \approx 65$ Å, contained 2×36 lipid molecules, and more than 2,000 molecules of water, in total approximatively 15,000 atoms. The complete system was equilibrated for 100,000 steps, with a timestep of 2 fs at a temperature of 317.5 K. During equilibration, a density profile and energy convergence of the system have been monitored. The resulting density profile is in very good agreement with the profiles reported earlier.[3,28]

2.2. Dissipative particle dynamics

Dissipative particle dynamics (DPD) is a relatively new simulation method, introduced in 1992 by Hoogerbrugge and Koelman.[29] By combining several aspects of molecular dynamics and lattice-gas automata, it captures hydrodynamic time and length scales much larger than can be reached with the first method and it avoids the lattice artifacts of the latter method. Hoogerbrugge and Koelman showed both by simulations and theoretical derivation that the DPD algorithm obeys the Navier–Stokes equations. The original scheme was modified in 1995 by Español and Warren[30] to ensure that a proper Boltzmann distribution is generated.

A DPD particle represents the center of mass of a cluster of atoms. The particles interact *via* a force consisting of three contributions, all of them pairwise additive. The total force on a particle i consists of a dissipation force $\boldsymbol{F}^{\mathrm{D}}$, a random force $\boldsymbol{F}^{\mathrm{R}}$, and a conservative force $\boldsymbol{F}^{\mathrm{C}}$, and can then be written as the sum of these forces:[29,31]

$$\boldsymbol{f}_i = \sum_{i \neq j} (\boldsymbol{F}_{ij}^{\mathrm{D}} + \boldsymbol{F}_{ij}^{\mathrm{R}} + \boldsymbol{F}_{ij}^{\mathrm{C}}) \tag{2.1}$$

The first two forces in eqn. (2.1) are of the form:

$$\begin{aligned} \boldsymbol{F}_{ij}^{\mathrm{D}} &= -\eta w^{\mathrm{D}}(r_{ij})(\hat{\boldsymbol{r}}_{ij} \cdot \boldsymbol{v}_{ij})\, \hat{\boldsymbol{r}}_{ij} \\ \boldsymbol{F}_{ij}^{\mathrm{R}} &= \sigma w^{\mathrm{R}}(r_{ij}) \zeta_{ij}\, \hat{\boldsymbol{r}}_{ij} \end{aligned} \tag{2.2}$$

where $\boldsymbol{r}_{ij} = \boldsymbol{r}_i - \boldsymbol{r}_j$ and $\boldsymbol{v}_{ij} = \boldsymbol{v}_i - \boldsymbol{v}_j$, with $\boldsymbol{r}_i$ and $\boldsymbol{v}_i$ representing the position and the velocity of particle i, respectively. η is the friction coefficient, σ the noise amplitude, and ζ_{ij} a random number taken from a uniform distribution, which is independent for each pair of particles. The combined effect of these two forces is a thermostat, which conserves (angular) momentum, and hence gives the correct hydrodynamics at sufficient long time and length scales.

Español and Warren[30] have shown that the equilibrium distribution of the system is the Gibbs–Boltzmann distribution if the weight functions and coefficients of the drag and the random force satisfy:

$$w^{\mathrm{D}}(r) = [w^{R}(r)]^2 \tag{2.3}$$

$$\sigma^2 = 2\eta k_{\mathrm{B}} T \tag{2.4}$$

The weight function $w^{\mathrm{R}}(r)$ is chosen as

$$w^{\mathrm{R}}(r) = \begin{cases} (1 - r/r_{\mathrm{c}}) & (r < r_{\mathrm{c}}) \\ 0 & (r \geq r_{\mathrm{c}}) \end{cases} \tag{2.5}$$

where r_{c} is the cut-off radius, which gives the extent of the interaction range. In this case, all forces assume the same functional dependence on the interparticle distance $\boldsymbol{r}_{ij}$ as the conservative force $\boldsymbol{F}_{ij}^{\mathrm{C}}$, which is usually of the form

$$\boldsymbol{F}_{ij}^{\mathrm{C}} = \begin{cases} a_{ij}(1 - r_{ij}/r_{\mathrm{c}})\, \hat{\boldsymbol{r}}_{ij} & (r_{ij} < r_{\mathrm{c}}) \\ 0 & (r_{ij} \geq r_{\mathrm{c}}) \end{cases} \tag{2.6}$$

where the coefficient $a_{ij} > 0$ is a parameter expressing the maximum repulsion strength. The equations of motion are integrated with a modified velocity Verlet algorithm.[31]

$$\begin{aligned} \boldsymbol{r}_i(t + \Delta t) &= \boldsymbol{r}_i(t) + \Delta t \boldsymbol{v}_i(t) + \frac{1}{2}(\Delta t)^2 \boldsymbol{f}_i(t) \\ \tilde{\boldsymbol{v}}_i(t + \Delta t) &= \boldsymbol{v}_i(t) + \lambda \Delta t \boldsymbol{f}_i(t) \\ \boldsymbol{f}_i(t + \Delta t) &= \boldsymbol{f}_i(\boldsymbol{r}_i(t + \Delta t), \tilde{\boldsymbol{v}}_i(t + \Delta t)) \\ \boldsymbol{v}_i(t + \Delta t) &= \boldsymbol{v}_i(t) + \frac{1}{2}\Delta t(\boldsymbol{f}_i(t) + \boldsymbol{f}_i(t + \Delta t)) \end{aligned} \tag{2.7}$$

in which $\tilde{\boldsymbol{v}}$ is a prediction for the new velocity $\boldsymbol{v}$. The original velocity–Verlet algorithm would be recovered for $\lambda = 0.5$. Groot and Warren explain in their paper[31] that the temperature can be controlled by three factors, the time step Δt, the noise level σ, and the λ in the Verlet algorithm. We use a density $\rho = 3$, $\sigma = 3$, $\lambda = 0.65$, and $\Delta t = 0.03$.

2.2.1. Reduced units. We use reduced units with r_{c} as the unit of length, the mass m of a particle as the unit of mass, and $a_{\mathrm{ww}} = 1$ as the unit of energy. The length scale depends on two factors in our mesoscopic simulation: the particle density ρ and the number of (water) molecules represented by one particle N_{m} (*e.g.* the mapping factor). The particle density ρ is the total number of DPD particles N_{w} divided by the volume V (in units of r_{c}^3): $\rho = N_{\mathrm{w}}/V$. The particle density and the mapping are used to define the value of r_{c}. For instance: we have N_{w} water beads in a volume V, then

$$\rho = N_{\mathrm{w}}/V = 1/v \tag{2.8}$$

where v is the volume in DPD units (r_{c}^3) of one DPD water particle. Let v' be the volume of one water molecule in Å^3 (= 30 Å^3), then we have:

$$v r_{\mathrm{c}}^3 = v' N_{\mathrm{m}} \tag{2.9}$$

replacing v by the expression of eqn. (2.8)

$$r_c = \sqrt[3]{v' N_m \rho} \tag{2.10}$$

If we take, for example, $N_m = 3$ and $\rho = 3$ as the level of coarse graining, then $r_c = 6.46$ Å and if we take $N_m = 1$ and $\rho = 3$, then $r_c = 4.48$ Å.

From this coarse-graining procedure, the interaction parameters are defined in units of k_BT. To use reduced units, we define $k_BT_0 = 1$ where T_0 is room temperature. The interaction parameters can then be expressed in these reduced units, *i.e.* the a_{ww} parameter has been fitted to give the correct compressibility of water at room temperature and at the assumed density. In principle, we could use the same procedure to match the compressibility of water at different temperatures. This gives, however, a temperature dependent a parameter which would make the interpretation of our results more complex. Therefore we have chosen to keep the parameters fixed and only change the temperature. In the following we will use the notation T^* to indicate the reduced temperature.

2.2.2. Tensionless bilayer. A biological membrane is not subject to external constraints and therefore adopts a tensionless configuration.[32] However, in most simulations of membranes one uses a fixed number of lipids and a fixed area, resulting in a membrane with a non-zero interfacial tension. To ensure that a tensionless bilayer is obtained, we performed simulations using an ensemble in which we can impose the surface tension. A Monte Carlo move, in which we change the area of the bilayer such that the total volume of the system remains constant, is performed after a randomly selected number of DPD steps. The move is accepted with a probability.[13]

$$\mathrm{acc}(o \rightarrow n) = \min\left(1, \frac{\exp[-\beta(U_n - \gamma A_n)]}{\exp[-\beta(U_o - \gamma A_o)]}\right) \tag{2.11}$$

where o and n indicate the old and the new configuration, respectively. U denotes the energy, γ the surface tension, A the area of the bilayer and $\beta = 1/k_BT$. In order to obtain the tensionless state of the bilayer γ is set to zero.

A typical simulation required 100,000 cycles of which 20,000 cycles were needed for equilibration. Per cycle it is chosen with a probability of 70% whether to perform 50 DPD time steps or to make an attempt to change the area of the box.

To ensure that, because the periodic boundary conditions, the bilayer–bilayer interactions do not influence the properties of a single bilayer, we selected the total number of water molecules such that the water layer thickness is sufficiently large that both bilayers are fully hydrated. This water layer thickness depends on the box size, which in turn is only known once the bilayer has adopted a state of zero tension. Therefore the number of water molecules was selected such that for the computation of the bilayer properties the minimum criterion was always met. For the self-assembly study we did study the formation of micelles, bilayers *etc.* as a function of the lipid concentration. For the bilayer we also investigated systems with a larger number of lipids, but we could not detect significant finite-size effects.

3. Coarse-grained models

3.1. Parameter sets

In DPD we have to choose the repulsion parameters such that the simulations yield the experimentally obtained values. In this section, we first summarize the method of Groot and coworkers,[5,31] in which the repulsion parameters are coupled to the Flory-Huggins χ-parameter. Then we give an overview of the parameter sets used by different researchers who studied the (phase) behavior of surfactants and phospholipids. On the basis of these parameters we define the sets used to perform the simulations in this paper.

Groot and Rabone published a data set, in which the compressibility of water is reproduced for a repulsion parameter $a_{ww} = 78$ at a reduced temperature of $T^* = 1$, a mapping factor $N_m = 3$, and the particle density $\rho = 3$.[5] To obtain the repulsion parameter of water at a different mapping factor, one can use:

$$a_{ii} = 78 k_B T \times N_m/\rho \tag{3.12}$$

To obtain the repulsion parameters for interactions between different types of beads, mutual solubilities of polymers in water can be used, expressed by the Flory–Huggins χ-parameters, which represent the excess free energy of mixing two species. There is a direct relationship between the Flory–Huggins χ-parameter and the excess repulsion Δa_{ij}.[5,31]

$$\chi = (0.231 \pm 0.001)\Delta a_{ij} \text{ if } \rho = 3 \tag{3.13}$$

a_{ij} can then be calculated with

$$a_{ij} = a_{ww} + \Delta a_{ij} \tag{3.14}$$

For most systems the Flory–Huggins χ-parameters are tabulated and eqns. (3.12) to (3.14) can be used to obtain the repulsion parameters. However, Flory–Huggins χ-parameters are determined for uncharged polymers, while phospholipids contain charged units.

With the mapping of three water molecules on one bead ($N_m = 3$), Groot and Rabone created the model of a phospholipid, depicted in Fig. 1. Using this mapping factor, one DPD-bead represents a volume of 90 Å^3. This volume also corresponds with the volume occupied by three methylene groups. The division of the lipid head group in three particles is estimated. Using the Flory–Huggins χ-parameters, Groot and Rabone obtained the set of parameters for this system as shown in Table 1. In this set the head groups are regarded as water with respect to the ester linkage and the hydrocarbon tails. In this approximation the head group is regarded as an ester group. For the values between brackets the charges of the head group are taken into account, leading to a reduced repulsion with water and an increased repulsion mutually. Groot and Rabone find that despite these different values, the density profiles are almost equal. Only the area per lipid changes from 62 Å^2 to 66.8 Å^2 if the charge of the head group is taken into account. Both values of the area per lipid are within the experimental range.[33]

One can also compare parameters used for ionic surfactants to obtain parameters for phospholipids. Table 2 shows the parameter set for ionic surfactants used by Groot.[12] In this set of parameters a different mapping is used: one water molecule

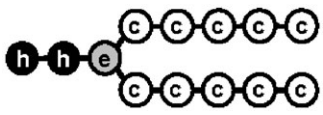

Fig. 1 The coarse graining of a phospholipid used by Groot and Rabone,[5] in which c represents a hydrophobic tail bead, e the ester linkage and h the hydrophilic head bead.

Table 1 Parameter sets used by Groot and Rabone[5]. For the values between brackets the charges of the head groups are also taken into account

a_{ij}	w	c	e	h
w	78	104	79.3	79.3 (75.8)
c	104	78	86.7	104
e	79.3	86.7	78	79.3
h	79.3 (75.8)	104	79.3	78 (86.7)

Table 2 Parameter set of Groot used for ionic surfactants[12]

a_{ij}	w	t	h
w	25	80	15
t	80	15	80
h	15	80	35

Table 3 Parameter set of Shillcock and Lipowsky[34]

a_{ij}	w	t	h
w	25	50	35
t	50	25	75
h	35	75	25

is mapped onto a single DPD particle. For this mapping the compressibility of water is reproduced using $a_{ww} = 25$ for $\rho = 3$ (see eqn. (3.12)). a_{hw} is lower compared to a_{ww} to mimic the hydration of a charged head group, and the increased value of a_{hh} represents the repulsion between charged head groups. The values of a_{ij} describing the hydrophobic interactions of the tail beads are not based on the Flory–Huggins parameters, but chosen to study the formation of micelles.

Shillcock and Lipowsky[34] investigated different models for a phospholipid with dissipative particle dynamics (see Table 3). They used a different parameter set in which on average a single tail bead represents three or four methyl groups. They suggest that the most simple model of a phospholipid contains one hydrophilic head bead with a single chain of hydrophobic segments. In this approach the single head bead represents the complete head group of a phospholipid. In a refinement of the model, the hydrophilic part contains more beads and the hydrophobic part contains two tails, varying in length. These tails are connected to two different beads of the head group. If the tails are connected to the same head bead no lamellar phase is found with this parameter set. Shillcock and Lipowsky also use a large angle bending potential to avoid interdigitation between the monolayers.

Ryjkina *et al.*[15] use DPD simulations to compute the phase behavior of non-ionic surfactants. In their model (see Table 4) the bead density equals 5 and therefore they divide the a_{ww} parameter by 5 to reproduce the compressibility of water at this particular density (see eqn. (3.12)). One molecule of DDAO (dodecyldimethylamine) is translated to a model which consists of one hydrophilic and one hydrophobic bead.

Clearly, this short overview illustrates that there is no unique set of mesoscopic parameters to describe phospholipid systems. Groot and Rabone[5] developed a systematic method to relate the repulsion parameters to the experimental system. This method implies that it is possible to translate parameters when a different level of coarse graining is applied. To investigate the sensitivity of the results on the details of the model, we define two independent sets of parameters. A third set is created by recalculating one set of parameters using eqns. (3.12) and (3.13). We apply these parameter sets on two mesoscopic models, which differ in the level of coarse graining.

These different parameter sets are listed in Table 5. Parameter set A is based on the simulations performed by Groot and Rabone,[5] with exclusion from a separate parameter for the glycerol linkage in the simulations. Parameter set B is based on the parameters used by Groot on calculations on surfactants.[12] We reduced the tail–tail interaction to avoid a very high density in the hydrophobic core. We obtained parameter set C from the repulsion parameters of Groot and Rabone.[5] By using eqns. (3.12) and (3.13), we obtain the parameters for a bead volume of 30 Å^3.

Table 4 Parameter set of Ryjkina *et al.*

a_{ij}	w	c	n
w	15	80	0
c	80	15	78
n	0	78	15

Table 5 Parameter sets used in our simulations. Parameter set A is based on the parameter set used by Groot for ionic surfactants[12] (see Table 2). Parameter sets B and C derived from the set used by Groot and Rabone[5] for bilayers (see Table 1)

A	w	t	h	B	w	t	h	C	w	t	h
w	25	80	15	w	78	104	75.8	w	25	34	24
t	80	25	80	t	104	78	104	t	34	25	34
h	15	80	35	h	75.8	104	86.7	h	24	34	29

3.2. Coarse-grained models

In this section, we present the two models used in the simulations. The volume per bead in model I is 30 Å^3 (corresponding with the mapping factor $N_m = 1$), while the bead volume of model II is 90 Å^3 ($N_m = 3$). In this section we discuss how we obtained a coarse-grained model of the phospholipid dimyristoyl phosphatidyl choline (DMPC). We show how the bond-bending potentials of the various angles are obtained from MD simulations. While these are results for a single tail length, it is very easy to change the lengths of the hydrophobic tails by adding or removing beads and their corresponding bond-bending potential.

3.2.1 Model I: $N_m = 1$. In the literature one can find applications with a mapping factor $N_m = 1$,[12] which corresponds to a coarse-grained level that is almost identical to a united atom model. One may wonder whether the use of the soft repulsion model is appropriate for this level of coarse-graining. To address this question, we created a model at this level of coarse-graining and we developed the model by defining additional intramolecular interactions between the beads.

At the mapping factor $N_m = 1$, we obtain the mapping shown in Fig. 3. To obtain this model we divide the DMPC in equal volumes of 30 Å^3, using the phospholipid component volumes determined by Armen *et al.*[35] Two consecutive beads are connected by harmonic springs with spring constant $k_r = 100.0$ and equilibrium distance $r_0 = 0.7$. To control the flexibility of the tails we add a harmonic bond-bending potential with bending constant k_ϕ and equilibrium angle ϕ_0.

Based on the method developed by Tschöpp *et al.*,[36] we obtained the values of k_ϕ and ϕ_0 by measuring the angular distribution function

$$P(\phi) = C\exp[-\beta(U(\phi))] \tag{3.15}$$

from all-atom MD simulations of a single phospholipid in water. This distribution is calculated using the center of mass of the cluster of atoms representing one bead. The parameters of k_ϕ and ϕ_0 were found by a quadratic fit of the data according to the relation:

$$\frac{1}{2}\beta k(\phi - \phi_0)^2 = -\ln P(\phi) \tag{3.16}$$

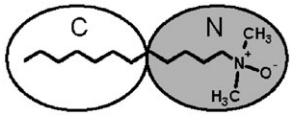

Fig. 2 Atomistic and DPD model of DDAO.

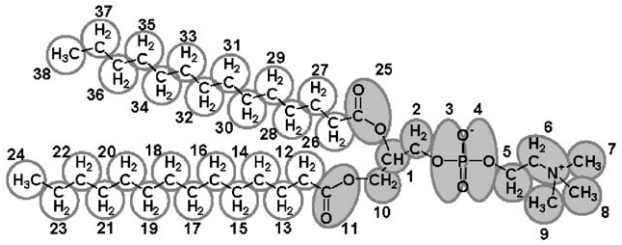

Fig. 3 The atomistic representation of DMPC and its corresponding coarse-grained model with a bead volume of 30 Å^3 (model I). White indicates a hydrophobic bead and grey indicates a hydrophilic bead.

In Fig. 4 the distribution of the angle ϕ, obtained from MD, and the curve fitting of the data are shown for the angle between three consecutive beads in the hydrocarbon chain. In Table 6 the values of the bond bending potentials are listed. The angle bending potentials of the angles in the tails are very well defined, which is to be expected, since the mapping of these hydrocarbon tails is equal to the united atom model. However, in the head group region, we cannot use the united atom approach and we find much more flexible angles. For some angles we observe a large distribution, which indicates a very flexible angle. For these angles we do not use a bond-bending potential.

Preliminary results showed that the resulting density profile of a bilayer consisting of these lipids does not resemble the density profile computed from MD simulations (results not shown). Therefore, we sought to improve the model by inserting additional angle-bending constants in the tails in which an angle is set between three non-consecutive beads $\phi_{i,i+2,i+4}$ (*e.g.* $\phi_{14\text{–}16\text{–}18}$, $\phi_{31\text{–}33\text{–}35}$). With the mapping procedure we found $k_\phi = 3.5$ and $\phi_0 = 180^\circ$ for these angles.

3.2.2 Model II: $N_m = 3$. If we use a mapping in which three water molecules are represented by a single DPD bead, we obtain the representation shown in Fig. 5. Again using the volumes determined by Armen *et al.*,[35] the mapping of the lipid using a bead volume of 90 Å^3 results in a model consisting of three hydrophilic head beads and two tails, each consisting of five hydrophobic tail beads. The same values for the spring constant and the equilibrium distance between two consecutive beads as in model I are used ($k_r = 100.0$ and $r_0 = 0.7$).

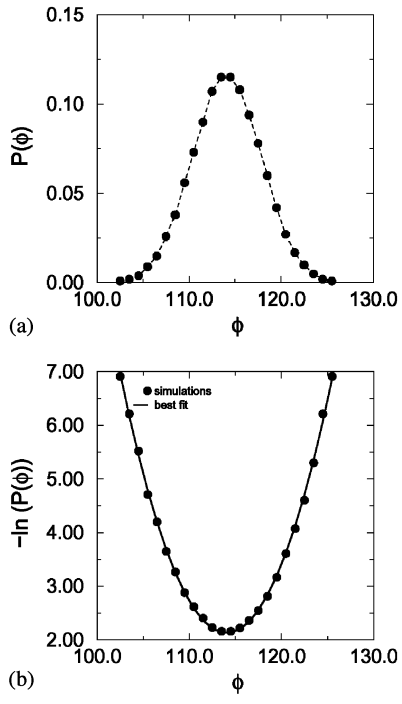

Fig. 4 Distribution (a) and fitting procedure (b) for the bond-bending potential of the angle between three subsequent beads in the tail ($\phi_{i,i+1,i+2}$).

Table 6 Parameters of model I. The angles between three consecutive beads in the tails (beads 11 to 24 and beads 25 to 38) are of type A. The remaining angles are very flexible and therefore a bond-bending potential is not used

ϕ	k_ϕ	ϕ_0
$\angle_{1\text{–}2\text{–}3}$	3.1	125°
$\angle_{2\text{–}3\text{–}4}$	4.3	127°
$\angle_{3\text{–}4\text{–}5}$	4.4	124°
$\angle_{4\text{–}5\text{–}6}$	1.3	131°
$\angle_{2\text{–}1\text{–}10}$	25	113°
$\angle_{1\text{–}10\text{–}11}$	9	143°
$\angle_{1\text{–}25\text{–}26}$	24	140°
$\angle_{10\text{–}11\text{–}12}$	23	140°
Type A	22	115°

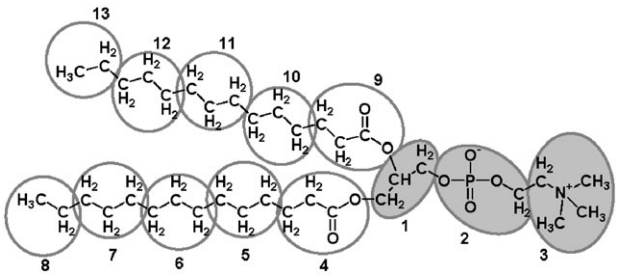

Fig. 5 The atomistic representation of DMPC and its corresponding coarse-grained model (model II). White indicates a hydrophobic bead and grey indicates a hydrophilic bead.

To obtain the values k_ϕ and ϕ_0 we followed the same procedure as for model I. However, due to the larger volume per bead and thus the higher number of atoms represented by one bead, the distribution of some angles is multimodal (see Fig. 6). To keep the simple harmonic potential, we repeated the MD simulations on a bilayer of DMPC to confirm that the selected equilibrium angle is the most abundant. The most abundant equilibrium angle ϕ_0 is used in subsequent simulations. In this way we obtained the values of k_ϕ and ϕ_0 listed in Table 7. The simulations show that the head group is completely flexible, and that the tails exhibit some order. Due to the larger volume per bead, a broader angle distribution is found for all angles compared to the results found for the angles of model I. As a result the values of k_ϕ are lower.

4. Results and discussion

In this section we compare the results from MD simulations with results of DPD simulations for the two models and the

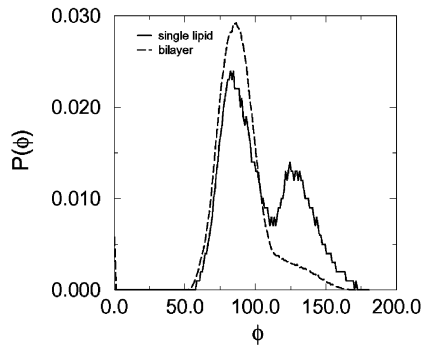

Fig. 6 Distribution of the angle $\phi_{4\text{–}1\text{–}9}$ obtained with MD-simulations of a single lipid in water and of a bilayer of DMPC.

Table 7 Parameters of model II. The angles ϕ_{4-5-6}, ϕ_{5-6-7}, ϕ_{6-7-8}, $\phi_{9-10-11}$, $\phi_{10-11-12}$, and $\phi_{11-12-13}$ are of type A and ϕ_{4-1-9} is of type B. The remaining angles are not set, meaning that the head group is completely flexible

$\phi_{0,A}$	180°
$k_{\phi 0,A}$	6
$\phi_{0,B}$	90°
$k_{\phi 0,B}$	3

parameter sets defined in Table 5. The quantities to compare are the area per lipid A_l, the hydrophobic thickness D_c of the bilayer, and the bilayer thickness D_b. These quantities can also be obtained experimentally by X-ray and neutron diffraction studies, and volumetric measurements (see for instance ref. 37). We also compare density profiles in the direction of the bilayer normal.

4.1. Model I: bead volume 30 Å^3

We used DPD to compute the properties of a bilayer of DMPC in water with model I (30 Å^3 bead size) and parameter set A. Starting from a random configuration of 200 lipids in 16200 water beads at a temperature $T^* = 1.0$ a bilayer was formed. Applying the zero surface tension scheme showed that this bilayer was stable.

Fig. 7(a) shows the density profiles of the MD-simulation, in which the atoms are translated to the corresponding beads, and of the DPD-simulation (Fig. 7(c)). The snapshots of the bilayer show that in the MD-simulation the final beads are located near the mid plane of the bilayer (Fig. 7(b)), while in the DPD simulation the terminal beads are more spread throughout the hydrophobic region (Fig. 7(d)). This is also reflected in the curves representing the CH_3-group; whereas in the MD density profile this curve is a narrow peak around the bilayer mid plane, the curve in the DPD density profile is almost constant across the hydrophobic core. The curves representing the CH_2-groups support this conclusion. In the MD density profile we observe a clear minimum at the bilayer mid plane, while this minimum is absent in the DPD density profile.

The curve representing the ester linkage obtained with the DPD simulation is in good agreement with the curve obtained with the MD simulation. In both profiles the peaks of these curves are located in the water and also surrounded by the hydrophobic core of the bilayer. The fact that in DPD the COO is not completely within the hydrophobic core, while this is the case in the MD simulation, is due to the strong repulsion between the hydrophobic and hydrophilic particles in the DPD simulations.

A remarkable difference can be observed from the curves representing the beads of the head group. The density profile of the MD simulation shows two 'Gaussian' curves for the choline group and phosphate group, which are overlapping and near the interface. The density profile of the DPD simulations shows that the head group is much more hydrated: the density of water is higher and the head group is more stretched, leading to a clear separation of the beads representing the choline and the phosphate group. Where in the MD simulations the hydrophobic region has the largest contribution to the bilayer thickness, in the DPD simulations the contributions of the hydrophilic part and the hydrophobic part are almost equal, *i.e.* in DPD the hydrophilic tendency of the head is overrepresented.

Quantitatively the results from the simulations approach the experimentally observed values. We find for the area per lipid and the hydrophobic thickness 55 Å^2 and 32 Å, respectively, while experimentally 60 Å^2 and 25.6 Å is found.[38]

It is interesting to create a new parameter set by recalculating parameter set B, created for a bead volume of 90 Å^3, to obtain a set for bead volume 30 Å^3. With the resulting parameter set C we performed simulations on 200 lipids in water. Starting from

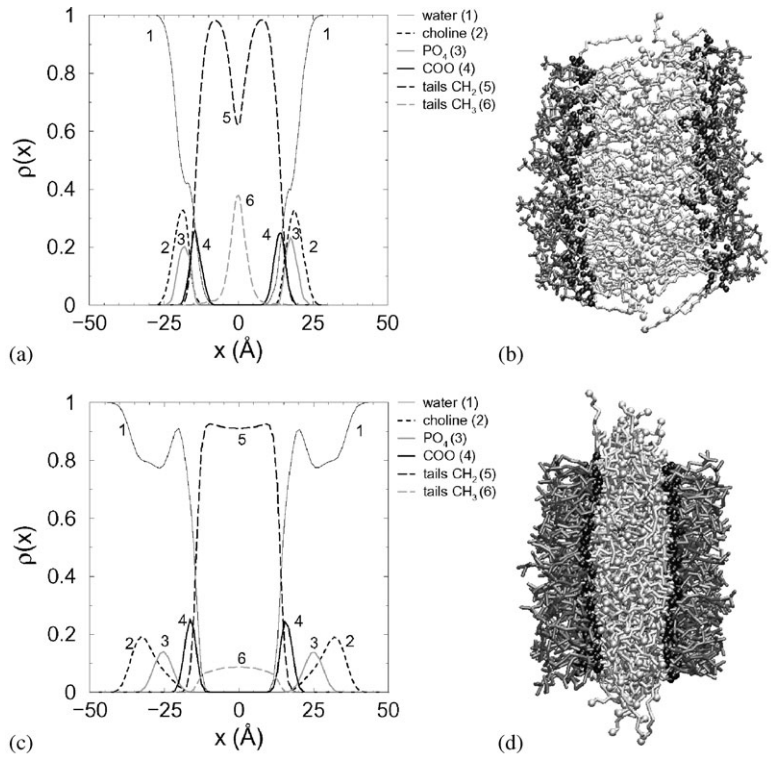

Fig. 7 Density profiles (a) and (c) and snapshots (b) and (d) of a bilayer of DMPC in water computed from MD simulations using the centers of mass as defined in Fig. 3 and DPD, using model I, respectively. In the density profiles (a) and (c) choline represents the sum of beads 6, 7, 8, and 9, PO_4 is the sum of beads 3 and 4, COO the sum of beads 11 and 25, the terminal CH_3 the sum of beads 24 and 38, and CH_2 the sum of the remaining hydrophobic beads (see Fig. 3). In (b) and (d) dark grey represents the head groups, the black spheres represent the ester groups, and light grey represents the hydrocarbon tails, of which the tail ends are indicated by a sphere. For colour versions see the supplementary information.†

a random configuration, no bilayer was formed. Most lipids assemble in a cluster, with water included in the hydrophobic core. Even if we take a bilayer as the initial configuration and perform the zero surface tension simulations the bilayer breaks up in a cluster of lipids, also containing water in the hydrophobic core and free lipids in the water phase.

4.2. Model II: bead volume 90 Å^3

With model II we performed simulations on 800 lipids with on average 10000 water particles using parameter sets A and B. Fig. 8 shows the density profiles of the resulting bilayers. Fig. 8(a) shows the profile using the results of the MD simulations, and Fig. 8(b) and 8(c) shows the profiles of bilayers computed from DPD simulations using parameter sets A and B, respectively.

In all profiles the glycerol linkage (bead 1 in model II, see Fig. 5) is located at the interface and the head groups are pointing into the water. The main difference in the density profiles obtained with the DPD simulations is that with parameter set A (Fig. 8(b)) the peaks are somewhat higher and narrower than with parameter set B (Fig. 8(c)). On the whole, however, the density profiles obtained with both parameter sets are in good agreement with the density profile obtained with the MD simulation. The terminal beads of the tails are located around the bilayer mid plane and are on average on the mid plane of the bilayer. This is also reflected in the curve representing the CH_2 groups of the tails, which shows a minimum at the bilayer mid plane. The glycerol linkage, which is the bead connecting the two tails (bead 1 in Fig. 5), forms the separation between the hydrophobic core and the water plus head groups. Both the curve of the density of the tail beads and the curve of the density of water cover this peak. Finally, the head groups point into the water and are clearly separated from the hydrophobic core.

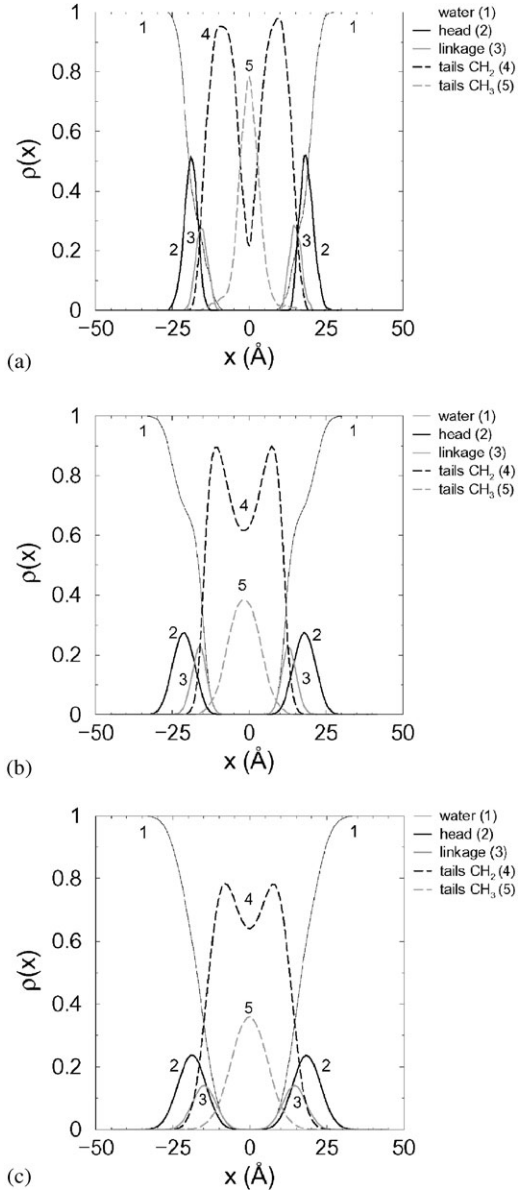

Fig. 8 Density profiles of a bilayer computed from MD simulations using the centers of mass as defined in Fig. 5(a), and of a bilayer formed by lipids coarse grained according to model II obtained from DPD simulations using parameter sets A (b) and B (c).

The difference between the profiles is the height of the peaks: with MD simulations the peaks are higher and narrower than with DPD simulations. The same difference can be noticed comparing the density profiles of the DPD simulations with parameter sets A and B. This indicates that the bilayer obtained with MD simulations is more ordered than the bilayer obtained with DPD simulations, parameter set A giving a more ordered bilayer than parameter set B.

Quantitavely, both parameter sets A and B give the same results for the area per lipid and the hydrophobic thickness. In our simulations we find at $\gamma = 0$, $A_l = 67$ Å^2 and $D_c = 29$ Å, which are both within the experimental range.

Comparing the results from model I with model II shows that a higher level of coarse graining leads to a better correspondence between MD and DPD simulations. It is necessary to coarse grain a phospholipid to a higher level than a level in which one particle represents only one water molecule. The reason is that in DPD each particle represents a cluster of atoms. The soft interactions in DPD allow these particles to overlap. If the particle size approaches a united-atom model size, as in model I, overlap of the particles is no longer realistic and soft potentials can no longer be used.

Using a higher mapping factor N_m, in which one DPD particle represents three water molecules or methylene groups, it is possible that particles do overlap. At this level a soft potential can be applied. This is clear from the density profiles; using a higher level of coarse graining gives the doubly peaked curve for the CH_2-group and a distribution of the tail ends around the mid plane of the bilayer, as was found both experimentally and by MD simulations.

4.3. Changing temperature and lipid topology

In the previous sections we discussed results obtained at a reduced temperature $T^* = 1.0$. At this temperature the bilayer is in the liquid crystalline or L_α phase, also called the liquid phase. We showed in the previous section that results obtained from model II agreed well with MD and experimental results. In this section we study the behavior of model II at a lower temperature. Experimentally, it is observed that the low temperature phase is the gel or $L_{\beta'}$ phase. In this phase the tails are ordered and show a collective tilt with respect to the bilayer normal. The head groups and the water surrounding the head groups are still fluid. Further we discuss briefly what is happening if the topology of the coarse-grained model changes by varying the length of the hydrophobic tails.

4.3.1 Changing temperature. Fig. 9(a) shows a bilayer consisting of model II lipids at a temperature of $T^* = 0.3$. From this snapshot it is clear that at this low temperature the bilayer is much more ordered than at temperature $T^* = 1.0$. The tails are straightened and ordered and show a tilt with respect to the bilayer normal. In Fig. 9(b) we show the two dimensional radial distribution functions of various particles in the plane of the bilayer. These curves show that the hydrophobic region is a very structured lipid. Due to the ordering of the tails the head

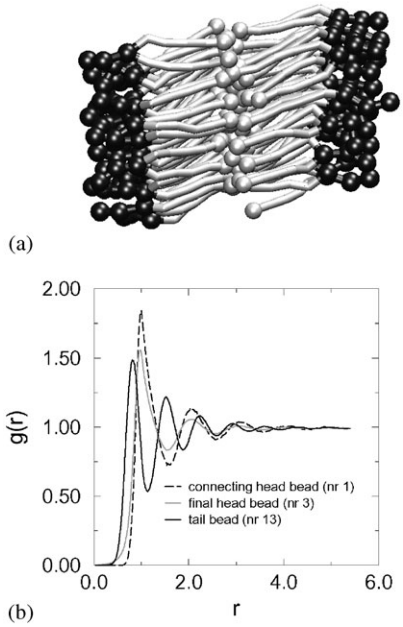

Fig. 9 (a) Snapshot of a DPD bilayer at $T^* = 0.3$ and (b) the two dimensional radial distribution functions of the final head bead, the bead connecting the two tails and a tail bead (bead 3, 1, and 13 in Fig. 5 respectively) in the plane of the bilayer. In (a) black represents the hydrophilic head group and grey the hydrophobic tails. The terminal beads of the tail are depicted by a grey sphere. For colour versions see the supplementary information.†

groups are more localized, but the radial distribution functions of the beads in the head group show that the bilayer as a whole and the surrounding water are still fluid. This allows us to apply the zero surface tension scheme.

The phase found at this temperature resembles very well the experimentally observed $L_{\beta'}$ phase. Experimentally[39,40] a tilt angle of $\theta = 32^\circ$ is observed, while we find a tilt angle of $\theta = 27^\circ$ for parameter set A and $\theta = 18^\circ$ for parameter set B. For the area per lipid we find $A_l = 46.6$ Å^2 and $A_l = 43.4$ Å^2 for parameter sets A and B, respectively, while the experimental value is $A_l = 47.2$ Å^2.[40] The hydrophobic thickness deviates significantly from the experimental value of $D_c = 30.3$ Å;[40] for parameter set A we find $D_c = 43.4$ Å and for B $D_c = 45.5$ Å. The two parameter sets lead to a different temperature at which the transition from the L_α to the $L_{\beta'}$ phase takes place. For parameter set A the transition temperature is found at $T^* = 0.35$, while for parameter set B a value of $T^* = 0.65$ is found.

4.3.2 Changing lipid topology. There are several ways to change the topology of the coarse grained lipid. One is to vary the length of the hydrophobic tails by adding or removing a tail bead. Simulations at $T^* = 1.0$ show that at zero surface tension the area per lipid is constant with increasing tail length from 4 to 7 beads. The hydrophobic thickness increases linearly with increasing tail length, both experimentally and in our simulations.[38,41]

Experimentally it is found that at the melting temperature the area per lipid as a function of tail length is constant.[41] However, the experimental data show large fluctuations in the area per lipid. A detailed study at a fixed temperature above the melting temperature, shows that the area per lipid decreases slightly, going from a tail length of 14 to a tail length of 18 carbons.[38] This decrease is attributed to the larger inter chain van der Waals interactions among the longer tails. In Fig. 10 we plot the area per lipid in Å^2 as a function of number of carbons in the tails of both the experimental and the computed values. Using the mapping factor $N_m = 3$ and parameter set A, we found that with fully flexibletails (*i.e.* no bending potentials) the area per lipid actually rose with increasing tail length. After

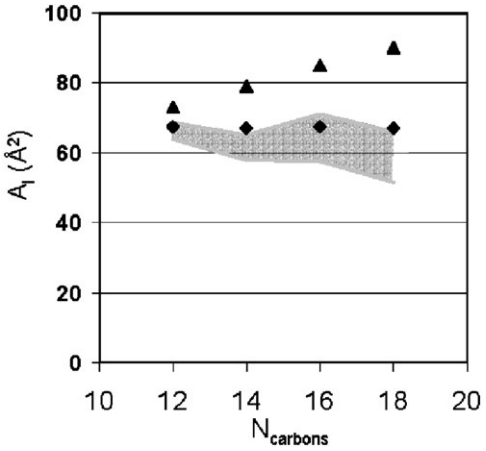

Fig. 10 Comparison of the experimental and computed values of the area per surfactant as a function of tail length. The computed values are represented by the black symbols and are calculated at a temperature $T^* = 1.0$. At this temperature, all bilayers are in the fluid L_α phase. The triangles are the values obtained with fully flexible model and the diamonds represent the values obtained with the model with additional bond-bending potentials. The grey area indicates the range of the experimentally obtained values.[38,41,43–46]

introduction of bending potentials the area per surfactant is constant within the error ($\Delta A_l/A_l = 5\%$), in agreement with the experimental results. The observed decrease in area per surfactant by Petrache *et al.*[38] is too small to allow for a detailed comparison with our mesoscopic model.

4.4. Driving forces in the formation of a bilayer

By comparing simulations with the three different parameter sets (see Table 5) we are able to pinpoint the repulsion parameters that are important in the self-assembly of a bilayer. In this section we discuss the choice of the repulsion parameters combined with the level of coarse graining.

To obtain a bilayer with DPD, we must have a phospholipid with clear hydrophobic and hydrophilic parts. The hydrophilic part sticks into the water phase, while the hydrophobic tails shield the core from the water particles. The parameter determining this shielding is a_{wt}. Too low a value for this parameter and water penetrates the core. As a result, no bilayer is formed as one saw from the simulations on model I, parameter set C (see section 4.1). In section 3.1 we assumed by combining eqns. (3.12) and (3.14) that a_{ii} can be calculated for every combination of N_m and ρ. The above results indicate, however, that one set of parameters cannot be translated straightforwardly into the other using these equations. Since the hydrophobic core of the cluster contains water and lipids can diffuse into the bulk water, it can be concluded that the repulsion between water and the hydrophobic tail segments a_{wt} is too low. This shows that the choice of parameters depends on the coarse graining level of the lipid in a more complex way than just a linear relation.

However, the scale to which water will penetrate the hydrophobic core depends not solely on the size of a_{wt}, but also on the interactions between the water particles themselves. Thus we expect that a large difference between a_{ww} and a_{wt} will favor the formation of a bilayer, while relatively low values of this difference allow for free mixing of water particles and tail beads. This is indeed borne out by the results presented in sections 4.1 and 4.2. For parameter sets A and B where $|a_{ww} - a_{wt}| = 55$ and $|a_{ww} - a_{wt}| = 26$ respectively, a bilayer was formed, while for parameter set A with $|a_{ww} - a_{wt}| = 9$ a bilayer could not form. Also the results from model II indicate that the difference between a_{ww} and a_{wt} is of importance. Both for parameter sets A and B a stable bilayer is formed and within the accuracy of our data the area per lipid A_l is equal.

Another important parameter that can influence the stability of the bilayer is a_{hw}, which determines the hydration of the head group. As was indicated by Groot and Rabone[5] the Flory–Huggins χ-parameter is not known for the head groups. They compare two parameter sets, in which the head group–water interaction is changed, resulting in a change in area per lipid but equal density profiles. For model II and parameter set A we changed a_{hw} from 15 to 25. The main effect is on the area per lipid; for $a_{hw} = 15$ $A_l = 67$ Å^2, while for $a_{hw} = 25$ $A_l = 63$ Å^2, which are both within the experimental range. Increasing this repulsion parameter to even higher values seems not a logical choice, since both the phosphate group and the nitrogen are charged units in the head group. This charge will result in the hydration of the head group, which can be translated in DPD by a lower value of a_{hw} compared to a_{ww}.

5. Conclusions

In this work, we compared the results from DPD simulations on coarse-grained models of a phospholipid with atomistic MD simulations. We created two mesoscopic models of DMPC, which differ in their level of coarse graining. Model I has a mapping factor of $N_m = 1$ with a volume of 30 Å^3 per bead and model II has a mapping factor of $N_m = 3$ with a volume of 90 Å^3. We found that we could correctly reproduce tail length dependency of both area per lipid and hydrocarbon core thickness, if we include bond-bending potentials in our model. We used results from MD simulations to obtain the bending constants and equilibrium angles.

This work shows that DPD is a powerful method to study the self-assembly of the lipids in a bilayer. It can be used to obtain qualitative dependence on temperature and length of the hydrophobic tail if a DPD bead represents a sphere with a volume of 90 Å^3. At the reference temperature of $T^* = 1.0$, where the bilayer is in the fluid L_α phase, the resulting density profiles of the MD and DPD simulations are in good agreement. At this temperature we can also reproduce the experimental values of area per lipid and the hydrophobic thickness. In ref. 42 we use such a mesoscopic model to study the effect of alcohol on the properties of a membrane. Lowering the temperature gives us the experimentally observed $L_{\beta'}$ phase, in which the tails are ordered and show a tilt with respect to the bilayer normal. Using a lower value of the mapping factor is not useful, because the soft repulsive potential used in DPD allows the beads to overlap, while overlap is not realistic in an (almost) atomic system.

Groot and Rabone[5] have studied in detail the relation between an MD time step and a time step used in a coarse-grained simulation. There are two combined effects that lead to a significant speed-up. Because of the soft potential the molecules can escape easier from a ''cage'' of surrounding molecules, which enhances the diffusion by three orders of magnitude. A second effect is related to the scaling of the physical parameters, the length scale is larger and also the total number of particles is reduced. This effect depends on the details of the coarse graining and scales as $N_m^{8/3}$ where N_m is the level of coarse graining.[5] These combined effects make model I about 3 orders of magnitude more efficient while for model II 4 orders of magnitude can be gained.

The results obtained with model I show that it is not possible to recalculate one parameter set into another one, if at the same time the level of coarse graining is changed. The assumption that a_{ii} can be calculated for every combination of N_m and ρ is too simple: the choice of the parameters depends not only on the level of coarse graining of the lipid. Also, a minimum difference between water–water and the water–hydrophobic tail repulsion parameters is needed if a lipid bilayer is to be formed. If the difference between this parameters is too small, the hydrophilic and the hydrophobic particles will not be completely separated and other structures than a bilayer are observed.

Acknowledgements

This work has been made possible by financial support of the Dutch chemical research council (NWO-CW).

References

1 K. M. Merz, Jr. and B. Roux, *Biological membranes: a molecular perspective from computation and experiment*, Birkhäuser, Berlin, 1996.
2 S. J. Marrink, E. Lindahl, O. Edholm and A. E. Mark, *J. Am. Chem. Soc.*, 2001, **123**, 8638–8639.
3 P. B. Moore, C. F. Lopez and M. L. Klein, *Biophys. J.*, 2001, **81**, 2484–2494.
4 R. Goetz and R. Lipowsky, *J. Chem. Phys.*, 1998, **108**, 7397–7409.
5 R. D. Groot and K. L. Rabone, *Biophys. J.*, 2001, **81**, 725–736.
6 J. C. Shelley and M. Y. Shelley, *Curr. Opin. Colloid Interface Sci.*, 2000, **5**, 101–110.
7 J. C. Shelley, M. Y. Shelley, R. C. Reeder, S. Bandyopadhyay and M. L. Klein, *J. Phys. Chem. B*, 2001, **105**, 4464–4470.
8 G. Ayton and G. A. Voth, *Biophys. J.*, 2002, **83**, 3357–3370.
9 L. Saiz and M. L. Klein, *Acc. Chem. Res.*, 2002, **35**, 482–489.
10 C. F. Lopez, P. B. Moore, J. C. Shelley and M. L. Klein, *Comput. Phys. Commun.*, 2002, **147**, 1–6.
11 J. C. Shelley, M. Y. Shelley, R. C. Reeder, S. Bandyopadhyay, P. B. Moore and M. L. Klein, *J. Phys. Chem. B*, 2001, **105** 9785–9792.
12 R. D. Groot, *Langmuir*, 2000, **16**, 7493–7502.
13 M. Venturoli and B. Smit, *PhysChemComm.*, 1999, **2**, 45.
14 S. Jury, P. Bladon, M. Cates, S. Krishna, M. Hagen, N. Ruddock and P. Warren, *Phys. Chem. Chem. Phys.*, 1999, **1**, 2051–2056.
15 E. Ryjkina, H. Kuhn, H. Rehage, F. Müller and J. Peggau, *Angew. Chem. Int. Ed.*, 2002, **41**, 983–986.
16 J. C. Shillcock and R. Lipowsky, *J. Chem. Phys.*, 2002, **117** 5048–5061.
17 S. Yamamoto, Y. Maruyama and S. Hyodo, *J. Chem. Phys.*, 2002, **116**, 5842–5849.
18 C. M. Wijmans and B. Smit, *Macromolecules*, 2002, **35** 7138–7148.
19 M. Kranenburg, M. Venturoli and B. Smit, *Phys. Rev. E*, 2003, **67**, art. no. 060901.
20 M. Kranenburg, M. Venturoli and B. Smit, *J. Phys. Chem. B*, 2003, **107**, 11491–11501.
21 Dlpoly 2.12, 2001.
22 A. D. MacKerell, Jr., D. Bashford, M. Bellott, R. L. Dunbrack, Jr., J. D. Evanseck, M. J. Field, S. Fischer, J. Gao, H. Guo, S. Ha, D. Joseph-McCarthy, L. Kuchnir, K. Kuczera, F. T. K. Lau, C. Mattos, S. Michnick, T. Ngo, D. T. Nguyen, B. Prodhom, W. E. Reiher, III, B. Roux, M. Schlenkrich, J. C. Smith, R. Stote, J. Straub, M. Watanabe, J. Wiórkiewicz-Kuczera, D. Yin and M. Karplus, *J. Phys. Chem. B*, 1998, **102**, 3586–3616.
23 W. L. Jorgensen, J. Chandrasekhar, J. D. Madura, R. W. Impey and M. L. Klein, *J. Chem. Phys.*, 1983, **79**, 926–935.
24 J. P. Ryckaert, G. Ciccotti and H. J. C. Berendsen, *J. Comput. Phys.*, 1977, **23**, 327–341.
25 U. Essmann, L. Perera, M. L. Berkowitz, T. Darden, H. Lee and L. G. Pedersen, *J. Chem. Phys.*, 1995, **103**, 8577–8593.
26 W. G. Hoover, *Phys. Rev. A*, 1985, **31**, 1695–1697.
27 M. P. Allen and D. J. Tildesley, *Computer Simulation of Liquids*, Clarendon Press, Oxford, 1989.
28 S.-W. Chiu, M. Clark, S. Subramaniam, H. L. Scott and E. Jakobsson, *Biophys. J.*, 1995, **69**, 1230–1245.
29 P. J. Hoogerbrugge and J. M. V. A. Koelman, *Europhys. Lett.*, 1992, **19**, 155–160.
30 P. Español and P. Warren, *Europhys. Lett.*, 1995, **30**, 191–196.
31 R. D. Groot and P. B. Warren, *J. Chem. Phys.*, 1997, **107** 4423–4435.
32 F. Jähnig, *Biophys. J.*, 1996, **71**, 1348–1349.
33 J. F. Nagle and S. Tristram-Nagle, *Curr. Opin. Struct. Biol*, 2000, **10**, 474–480.
34 H. Shinto, M. Miyahara and K. Higashitani, *Langmuir*, 2000, **16**, 3361–3371.
35 R. S. Armen, O. D. Uitto and S. E. Feller, *Biophys. J.*, 1998, **75**, 734–744.
36 W. Tschöpp, K. Kremer, J. Batoulis, T. Bürger and O. Hahn, *Acta Polym.*, 1998, **49**, 61–74.

37 J. Katsaras and T. Gutberlet, *Lipid Bilayers. Structure and interactions*, Springer, Berlin, 2001.
38 H. I. Petrache, S. W. Dodd and M. F. Brown, *Biophys. J.*, 2000, **79**, 3172–3192.
39 S. Tristram-Nagle, R. Zhang, R. M. Suter, C. R. Worthington, W. J. Sun and J. F. Nagle, *Biophys. J.*, 1993, **64**, 1097–1109.
40 S. Tristram-Nagle, Y. Liu, J. Legleiter and J. F. Nagle, *Biophys. J.*, 2002, **83**, 3324–3335.
41 B. A. Lewis and D. M. Engelman, *J. Mol. Biol.*, 1983, **166**, 211–217.
42 M. Kranenburg and B. Smit, *FEBS Lett.*, 2004, **568**, 15–18.
43 L. J. Lis, M. McAlister, N. Fuller, R. P. Rand and V. A. Parsegian, *Biophys. J.*, 1982, **37**, 657–666.
44 R. P. Rand and V. A. Parsegian, *Biochim. Biophys. Acta.*, 1989, **988**, 351–376.
45 H. I. Petrache, S. Tristram-Nagle and J. F. Nagle, *Chem. Phys. Lipids*, 1998, **95**, 83–94.
46 J. F. Nagle and M. C. Wiener, *Biochim. Biophys. Acta*, 1988, **942**, 1–10.